The effects of nonlinear wave propagation on inertial cavitation

David Sinden, Eleanor Stride & Nader Saffari

Department of Mechanical Engineering
University College London

AFPAC 09

December 9th 2008

Outline

Motivation

- High intensity focused ultrasound (HIFU) can be used in the treatment of cancerous tumours.
- Cavitation can enhance treatment and provide a measure of temperature if modelled accurately.
- Ability to localise and control cavitation activity is crucial for the safety and efficacy of treatment.

Modelling Cavitation

Rayleigh-Plesset equation [Lauterborn, 1976][1]

$$\rho\left(\ddot{R}+\frac{3}{2}\dot{R}^{2}\right)=p_{g}\left(T,c\right)+p_{v}-p\left(t\right)-\frac{2\sigma}{R}-\frac{4\mu\dot{R}}{R}$$

The equation needs to be rederived in a number of ways to include

- Visco-elasticity
- Temperature and pressure
- Rectified diffusion
- Incident wave
- Multiple bubbles ...

[1] Lauterborn, W. *J. Acoust. Soc. Am.* (1976) **59** p. 283

Stability

There are a variety of terms and definitions for stability relating to cavitation

- Sensitivity to initial conditions (Mel'nikov analysis)
- Period doubling cascades
- Unbounded growth (escape oscillator)
- Blake critical radius

From a clinic perspective unpredictable motion is as potentially undesirable as unbounded bubble expansion.

Incident Wave

A solution to Burgers' equation

$$\frac{\partial p}{\partial t} + p\frac{\partial p}{\partial x} = \nu \frac{\partial^2 p}{\partial x^2}$$

from weak shock theory [Blackstock, 1964][2] yields

$$p\left(t\right) = \sum_{n=1}^{\infty} \frac{2}{nr} J_n\left(nr\right) \sin\left(n\omega t\right) = \sum_{n=1}^{\infty} p_n \sin\left(\omega_n t\right), \quad \omega_n = n\omega$$

where $r = \omega_0 \rho c / \beta p_0$, J_n is a Bessel function of order n and β is the standard 'nonlinearity' parameter.

[2] Blackstock, D. T., *J. Acoust. Soc. Am.* (1964) **36** p. 534

Incident Wave

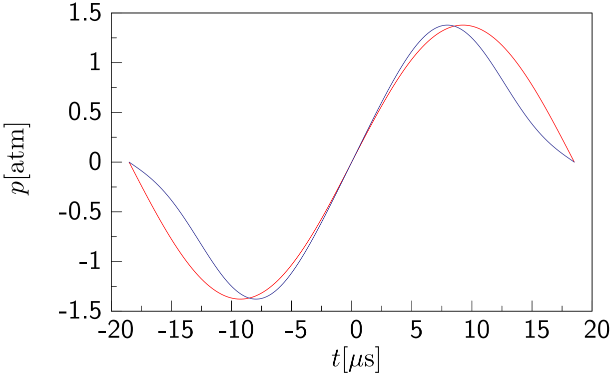

Figure: Profiles of distorted wave passing through a nonlinear medium (blue) and undistorted wave passing through a linear medium (red).

Distribution of harmonics

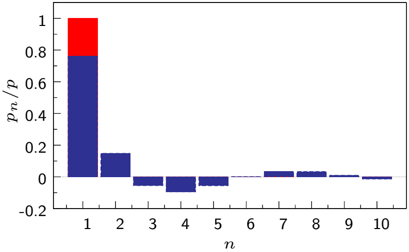

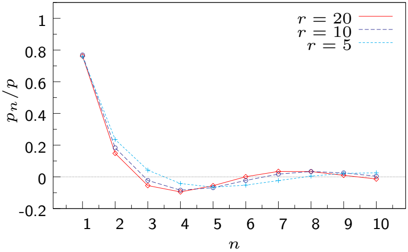

- Energy transfered from fundamental to higher harmonics.
- The further from a shock the smaller the contributions from higher harmonics, providing a less distorted wave profile.

Contrast in radius-time profiles

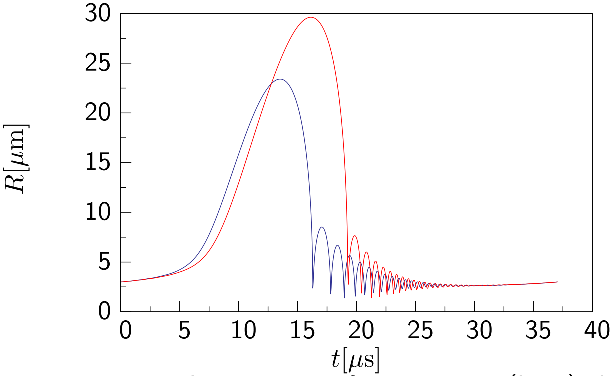

- Maximum amplitude $R_{\max}$ less for nonlinear (blue) than linear (red) wave propagation.
- Inertial cavitation occurs earlier in each cycle.

Period-Doubling Bifurcation

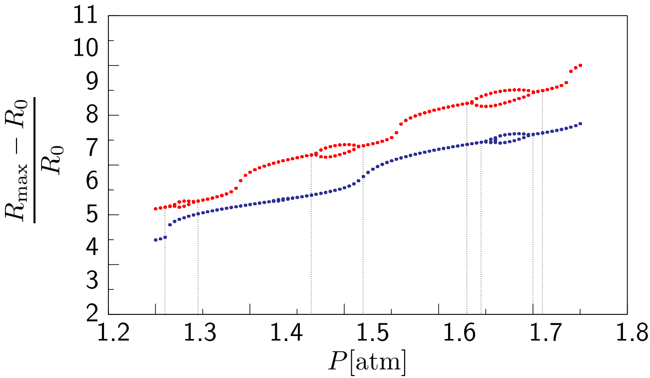

Figure: Bifurcation diagram for $R_0 = 0.80\mu$m when $\omega = 26.5$MHz illustrating that the period doubling bifurcations occur for smaller equilibrium radii or forcing pressures for linear waves (red) than nonlinear waves (blue)

Period-Doubling Bifurcation

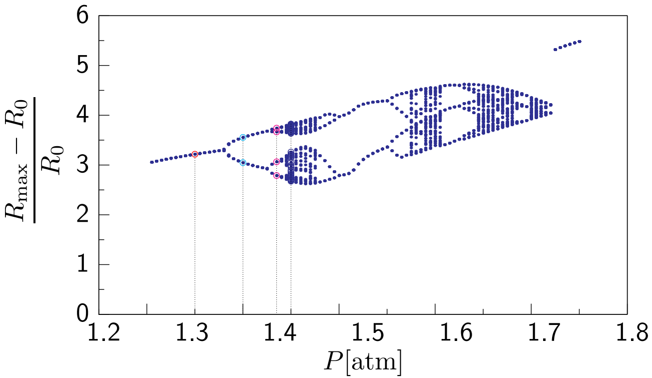

Figure: Bifurcation diagram for nonlinear wave with $R_0 = 1.40\mu$m when $\omega = 26.5$MHz illustrating the regions of stability. One-cycle are at $p =$1.300atm, two-period at 1.400atm, four-period at 1.435atm and by 1.450atm quasi-periodic oscillations

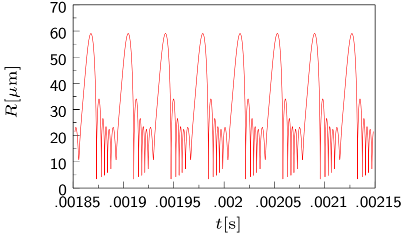
70
60
50
40
30
20
10
0
.00185
.0019
.00195
.002
.00205
.0021
.00215
$t\,[\mathrm{s}]$
$R\,[\mu\mathrm{m}]$

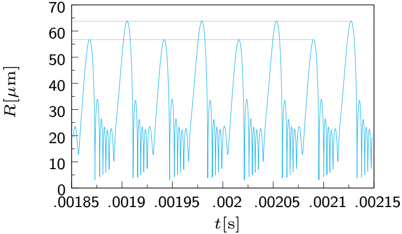
70
60
50
40
30
20
10
0
.00185
.0019
.00195
.002
.00205
.0021
.00215
$t\,[\mathrm{s}]$
$R\,[\mu\mathrm{m}]$

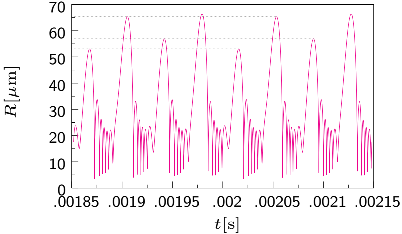
70
60
50
40
30
20
10
0
.00185
.0019
.00195
.002
.00205
.0021
.00215
$t\,[\mathrm{s}]$
$R\,[\mu\mathrm{m}]$

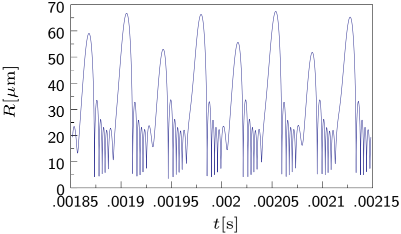
70
60
50
40
30
20
10
0
.00185
.0019
.00195
.002
.00205
.0021
.00215
$t\,[\mathrm{s}]$
$R\,[\mu\mathrm{m}]$

Fourier Analysis

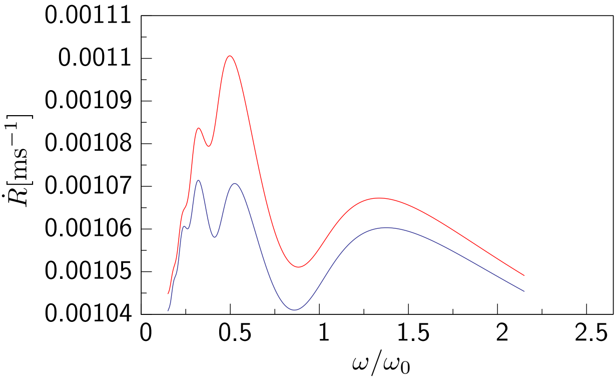

Figure: Frequency response curves for linear (red) and nonlinear (blue) wave propagation showing greater influence of ultra- and subharmonic components in nonlinear case.

Normal Form Analysis

Following [Harkin et al., 1999][3] and considering bubbles whose initial size R_0 is slightly below the critical Blake radius R_c by $R = R_0 \left(1 + \epsilon x \left(\tau\right)\right)$ where $\epsilon = 2\left(1 - R_0/R_c\right)$ then to $\mathcal{O}\left(\epsilon^2\right)$ yields

$$\ddot{x} + 2\zeta\dot{x} + x\left(1 - x\right) = \sum_{n=1}^{N} A_n\left(\tau\right)\sin\left(\bar{\omega}_n\tau + \tau_0\right).$$

where $\tau = \left(2\sigma\epsilon/\rho R_0^3\right)^{1/2} t$, $\zeta = \left(2\mu^2/\epsilon\sigma\rho R_0\right)^{1/2}$, $A_n = p_n R_0/2\sigma\epsilon^2$ and $\bar{\omega}_n = \omega\left(\rho R_0^3/2\sigma\epsilon\right)^{1/2}$ for a sufficiently large N.

[3] Harkin A., Nadim A. and Kupper, T. J. *Phys. Fluids* **11** p. 274

Mel'nikov Analysis

Using techniques from complex analysis, the Mel'nikov integral can be calculated explicitly. However no explicit formula for simple zeros which determines a threshold for 'chaotic' dynamics exists!

$$\mathcal{M}\left(\tau_0\right) = \sum_{n=1}^{N} \frac{6\pi A_n \bar{\omega}_n^2 \cos\left(\bar{\omega}_n \tau_0\right)}{\sinh\left(\pi \bar{\omega}_n\right)} - \frac{12\zeta}{5}$$

Numerics show that instability of the distorted wave occur at greater values of the forcing than for undistorted waves.

Conclusions

- As first harmonic is reduced there is a reduction in maximum amplitude: leading to
  - reduced likelihood of shape instability, either through Rayleigh-Taylor or parametric instability,
  - similarly reduced likelihood of shockwave formation.
- The earlier onset of collapse should allow a greater time for the bubble to return to an equilibrium radius and for stable inertial cavitation to occur: larger regimes of stable motion.
- Good agreement between stability results investigated numerically and analytically.

References

Blackstock, D. T. (1964).
Thermoviscous attenuation of plane, periodic, finite-amplitude sound waves.
J. Acoust. Soc. Am., 36:534.

Harkin, A., Nadim, A., and Kaper, T. J. (1999).
On acoustic cavitation of slightly subcritical bubbles.
Phy. Fluids, 11:274.

Lauterborn, W. (1976).
Numerical investigation of nonlinear oscillations of gas bubbles in liquids.
J. Acoust. Soc. Am., 59:283.